ARTICLE

Electrospinning of Poly(alkoxyphenylenevinylene) and Methanofullerene Nanofiber Blends

Harvey A. Liu, Danny Zepeda, John P. Ferraris,* and Kenneth J. Balkus, Jr.*

Department of Chemistry, The University of Texas at Dallas, 800 West Campbell Road, Richardson, Texas 75080-3021

ABSTRACT Poly(*p*-phenylenevinylene) (PPV) derivatives have long been studied because of their attractive opto- and electroluminescent properties and have potential applications for devices such as light-emitting diodes and photovoltaics. The ability to induce alignment of these PPV derivatives may lead to the enhancement of charge mobility and their efficiency. In this study, uniform nanofibers of poly[2,5-(2′-ethylhexyloxy)]-1,4-phenylenevinylene (BEH-PPV) have been fabricated through the method of electrospinning, and an induced alignment of the polymer fibers was observed through photoluminescence data. This study also focuses on the doping of these fibers with the fullerene derivative, 1-(3-methoxycarbonyl)-propyl-1-phenyl-(6,6)-C_{61} (PCBM), to induce more incidence of donor/acceptor junctions. Composite fibers with up to a 1:2 weight ratio of PCBM/BEH-PPV have been fabricated and exhibited an ability to quench the photoluminescence of BEH-PPV, indicative of charge transfer.

KEYWORDS: electrospinning • composite fibers • poly(alkoxyphenylenevinylene) • methanofullerene • phenyl-C_{61}-butyric acid methyl ester • photovoltaics

The method of electrospinning has been utilized in the fabrication of micrometer- to nanometer-sized fibers composed of various materials including polymers (1, 2), ceramics (3–11), conducting polymers (12–14), and composites (15), which have found application in areas such as tissue engineering (16, 17), catalysis (18), gas sensors (19), composite materials (15), supercapacitors (19, 20), drug delivery (21), as well as self-healing films (22). Electrospinning is a nonmechanical fiber-drawing method that applies electrostatic forces to a polymer melt or solution fed through a needle or spinneret, causing the polymer melt to form a Taylor cone and undergo a whipping action (2). The whipping motion induces a stretching of the polymer solution, increasing the surface-to-volume ratio and expediting the evaporation of the solvent, resulting in the formation of a nonwoven mat of submicrometer-sized fibers (2, 23, 24). Previous studies have demonstrated that the stretching forces associated with electrospinning may also induce orientation of the polymer chains along the length of the fiber (25–27). These characteristics make electrospinning a very attractive technique for devices utilizing conducting polymers, especially for poly(*p*-phenylenevinylene) (PPV) derivatives, where the alignment and charge mobility are integral in device performance (28, 29). In past studies, it was demonstrated that the induced alignment of these polymer chains may lead to higher charge-carrier mobility or polarized photoluminescence (PL) and increase the efficiency of an optoelectronic device (30, 31).

PPVs have long been studied because of their opto- and electroluminescent properties, which have potential applications for devices such as light-emitting diodes (LEDs) (32, 33) and photovoltaics (28, 34). This class of conjugated polymers is of particular interest because of its facile synthesis (35), its semiconductive properties due to delocalization of the π electrons along the polymer backbone, and its tunable optically emissive properties. While the parent polymer, poly(1,4-phenylenevinylene), is insoluble, it has been demonstrated that substituents with long alkyl chains can induce solubility and enhance processability of these polymers (36). The high thermal stability (T_d > 350 °C) and high elastic modulus of PPVs also contribute to an enhancement of its mechanical properties. These traits make PPVs attractive materials for plastic solar cells (PSCs) (37). Currently, high power conversion efficiencies up to 2.65% have been reported for PSCs consisting of the PPV derivative poly[2-methoxy-5-(3′,7′-dimethyloctyloxy)]-1,4-phenylenevinylene (MDMO-PPV) and 1-(3-methoxycarbonyl)-propyl-1-phenyl-(6,6)-C_{61} (PCBM), which were deposited via spin-casting (38). Unfortunately, the high PCBM to MDMO-PPV ratio (4:1) leads to large aggregates of PCBM within the active MDMO-PPV layer, contributes to the reduction of charge mobility, and thus limits the power conversion of devices based on these composites (28, 39).

We first reported the electrospinning of poly[2-methoxy-5-(2-ethylhexyloxy)]-1,4-phenylenevinylene (MEH-PPV) with silica mesoporous molecular sieves, though occasionally beaded leaflike structures were observed in the nonwoven fiber mats (40). The silica in this instance served as a spacer, reducing the interchain interactions that resulted in a blue shift of the emission wavelength maximum (λ_{max} = 566 nm)

* E-mail: ferraris@utdallas.edu (J.P.F.), balkus@utdallas.edu (K.J.B.).
Received for review May 17, 2009 and accepted July 30, 2009

DOI: 10.1021/am900338w

Published on Web 08/13/2009

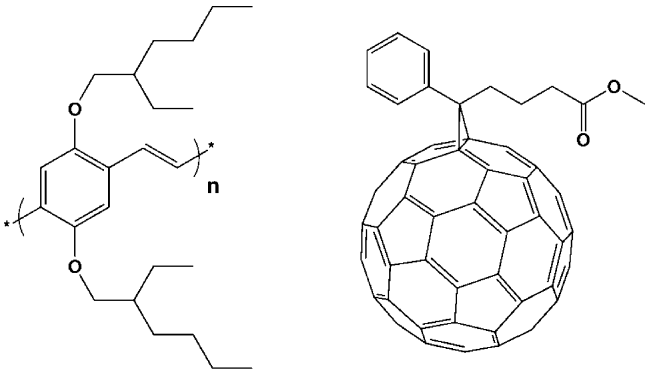

FIGURE 1. BEH-PPV and PCBM.

of the composite fibers relative to pure MEH-PPV fibers (λ_{max} = 599 nm) (40). We have also been able to electrospin neat fibers of MEH-PPV, poly[2-dimethyloctylsilyl]-1,4-phenylenevinylene (DMOS-PPV), and their blends with the aid of the surfactant Triton-X (41). The spun PPV fibers exhibited diameters ranging from 200 to 500 nm, showed very little signs of beading, and exhibited a red shift in their emission maxima compared to their solution emission spectra. We have also been able to electrospin blends of MEH-PPV and DMOS-PPV, which exhibited complete Forster-type energy transfer in PL studies (41). Others have shown the ability to make blends with MEH-PPV and a more readily spinnable polymer such as poly(vinyl alcohol) to attain a suitable polymer melt (42). More recently, MEH-PPV electrospun fibers with a core–shell structure were fabricated using concentric electrospinning (3, 26). This method allows one to fabricate nanofibers of polymers that are difficult to electrospin directly. The concentric method involves feeding a solution of MEH-PPV through the core surrounded by a sheath of poly(vinylpyrrolidone) (PVP) (26). Through this process, MEH-PPV nanofibers and ribbons with a consistent diameter size (~30 nm) were fabricated. However, extraction of the PVP was required and resulted in a nonuniform wrinkled fiber surface. Zhao et al. also employed concentric electrospinning, but in this case, MEH-PPV was the sheath material and PVP the core (43).

In the present study, uniform submicrometer-sized fibers of pure poly[2,5-(2′-ethylhexyloxy)]-1,4-phenylenevinylene (BEH-PPV; Figure 1a) were electrospun as a free-standing paper, without the use of a dual-capillary spinneret, a blended solution, or the use of a surfactant. The electrospun fibers exhibit a red-shifted PL, indicating increased interchain interactions between polymer chains due to an induced alignment. Additionally, the soluble C_{60} derivative, PCBM (Figure 1b), was incorporated within the fibers to possibly create a higher number of donor/acceptor junctions or sites, inducing higher photoinduced electron-transfer efficiency and increasing the number of charge percolation pathways. This polymer composite in fiber morphology is the first of its kind and may prove to be an improved active layer in photovoltaics (28, 44).

Electrospinning of Neat BEH-PPV Fibers Pure BEH-PPV fibers were electrospun from 3% solutions of BEH-PPV in a chloroform and methanol mixture with a ratio of 5:1 (v/v). First, the polymer was completely solubilized in chloroform, followed by the addition of methanol in the appropriate ratio. Upon the initial introduction of methanol into the polymer solution, a small portion of the polymer precipitated, but upon further stirring, the polymer again dissolved in the solvent system, yielding a homogeneous polymer solution. The BEH-PPV fibers electrospun from these solutions exhibited no beading through the use of this cosolvent system and displayed diameters ranging from ~100 to 250 nm. The frequency of bead formation was found to increase as the ratio of methanol to chloroform decreased. It has been previously demonstrated that, with the introduction of small amounts of a poor solvent, such as methanol, in a solution of MEH-PPV in a good solvent, such as chloroform or chlorobenzene, aggregation of the polymer chains occurs, resulting in the alignment of the polymer chains and an increase in the interchain interactions (45). This alignment of the polymer chains contributes to the spinability of the polymer solution and prevents the occurrence of beads throughout the fibers. Additionally, with the introduction of methanol, the viscosity of the polymer solution decreased significantly, which also decreases the surface tension of the polymer melt, resulting in an increase in the spinability of the polymer. Before the introduction of methanol, the viscosity of the polymer solution was measured at 2.75×10^3 cP s. The addition of methanol decreased the viscosity of the polymer solution to 1.00×10^3 cP s. Methanol also exhibits a higher dielectric constant than chloroform, which contributes to an increase in Coulombic repulsions, resulting in stretching of the fiber during the whipping stage of electrospinning and possibly reducing the amount of beading (2).

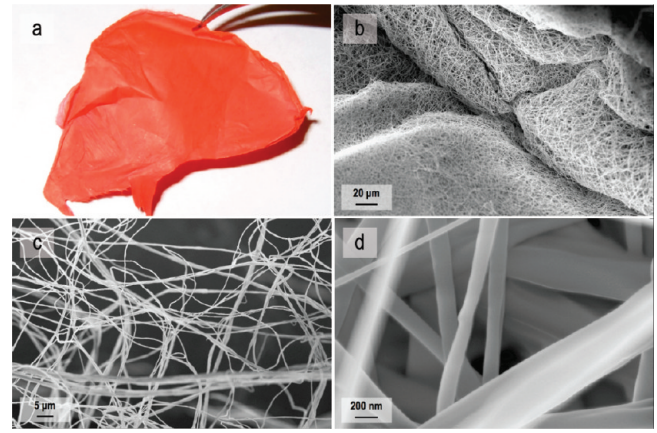

FIGURE 2. Pure electrospun BEH-PPV fibers: (a) digital image of as-spun electrospun fibers as a free-standing paper; (b–d) SEM micrographs of pure BEH-PPV electrospun fibers.

A digital image of the as-spun fibers as a nonwoven free-standing paper is shown in Figure 2a. The free-standing papers fabricated through this method were robust and could be easily handled and manipulated. Scanning electron microscopy (SEM) micrographs of these fibers are depicted in Figure 2b,c. The fibers electrospun from the 3 wt % solution of BEH-PPV ranged from ~100 to 250 nm in diameter, which was consistent throughout the sample. In

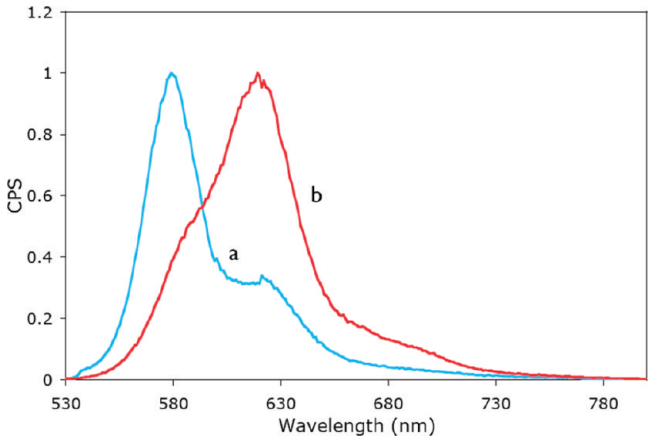

FIGURE 3. PL spectra of (a) the BEH-PPV film and (b) BEH-PPV electrospun fibers.

addition to the uniform diameter of these fibers, they also exhibited a smooth surface (Figure 2d), as opposed to the wrinkled surface seen in coaxially electrospun fibers demonstrated by Li et al. (26) The smooth surface was attributed to the use of conventional electrospinning, which did not utilize an outer sheath material to aid in fiber fabrication, omitting the need for extraction of the fibers. Conventional electrospinning also provides another benefit in that the incorporation of this material in a device could be easily implemented in a roll-to-roll process because no post-electrospinning steps are needed.

A toluene/methanol cosolvent system was also explored in the electrospinning of neat BEH-PPV. The concentration of BEH-PPV in toluene was kept at 3% (w/v), and the ratio of methanol was varied, but none of the prepared polymer solutions produced fibers through electrospinning. This could be attributed to the random-coil conformation that the polymer chain undergoes when dispersed within a solvent such as toluene, which may prevent interchain interaction along the length of the polymer chains, thus inhibiting the stretching of charged jets during the bending instability of electrospinning (46). One of the factors that contributes to the spinability of a polymer is its ability to entangle and interact along its polymer chain during the whipping stage, where elongation occurs. The entanglements that occur between the polymer chains allow for the physical stretching of the polymer melt without disjoining. While a random coil is the predominant conformation in toluene, in chloroform, BEH-PPV possesses a more elongated defect coil conformation (29). The elongated conformation allows for more entanglements and interactions of the polymer chains, permitting the stretching of the polymer melt during electrospinning.

Effect of Methanol on the Polymer Chains in Solution. With the introduction of the cosolvent methanol, the polymer chains begin to orient into aggregates, aligning along the length of the polymer, which may contribute to the ease of electrospinning of these polymers with this cosolvent system. The evidence of aggregate formation can be seen in the PL data. PL spectra of the as-spun pure BEH-PPV fibers and spun-cast thin films are shown in Figure 3. The BEH-PPV film profile shows an emission maximum at 580 nm, with a shoulder at 620 nm, which is similar in structure but red-shifted to its chloroform solution profile (solution emission at 558 and 607 nm) (47). The red shift is generally attributed to the extended conformation of the polymer chains caused by spin casting from a chloroform solution. The polymer conformation is maintained after the spin-casting process because of the fast evaporation of the solvent (48). The maximum emission at 580 nm indicates that the chromophores with the longest conjugation lengths represent the main type emitter, which is at 580 nm. The shoulder at 620 nm is generally attributed to aggregation, where the emission of excited π electrons relaxes because of the various vibronic energy levels of the electronic ground state (48, 49). Aggregations, as defined by Nguyen et al., refer to the alignment along the length of the polymer chains, resulting in interchain interactions (48). According to Nguyen et al., as the degree of interchain interactions increases, the overall luminescence decreases, yielding a material better able to transmit charge carriers between chains. This phenomenon results in a more efficient collection of charge through the polymer and reduces the losses from emissive recombination, enhancing polymer-based solar cell efficiencies (48).

In comparison, the BEH-PPV emission profile for the as-spun fibers (green) shows a maximum at 620 nm with shoulders at 590 and 695 nm. Electrospun PPV fibers previously reported by Li et al. have shown an emission profile similar to its thin film, i.e., with an emission maximum at 580 nm and the vibronic shoulder at 620 nm (26). It has been reported that the introduction of a poor solvent such as methanol causes the polymer chains to aggregate in order to minimize interaction with the poor solvent (45). In such a system, the good solvent−poor solvent miscibility reduces the hydrodynamic volume of the polymer chains, causing them to collapse, or aggregate, into a less thermodynamically favorable π-stacking conformation. This stacked conformation is maintained during the elongation of the polymer solution during the electrospinning process, although complete stretching of the polymer chain is not achieved, leading to the shoulder in the PL appearing at 590 nm from the main-type emitter. The red shift observed in the main-type emitter of the pure fibers can be attributed to the aggregation of the polymer chain, which reduces the torsional motion along the polymer backbone. The restriction of the polymer backbone reduced the rotational and vibrational energies along the backbone of the conjugated polymer, thus increasing the conjugation length (45). The shoulder appearing at 695 nm originates from single chromophore emissions because of energy transfer from a shorter conjugated to a neighboring longer conjugated segment (49).

Electrospinning of BEH-PPV/PCBM Composite Fibers. The chloroform/methanol solvent system used in the electrospinning of the neat BEH-PPV was used in the electrospinning of the PCBM composite fibers under an applied electrical potential of 15 kV over a fixed distance of

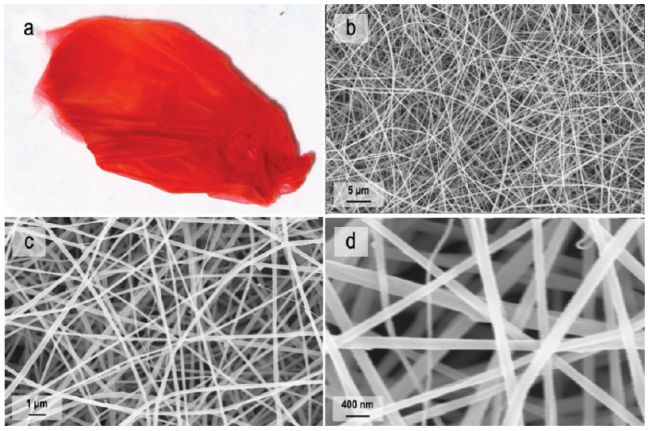

FIGURE 4. 1:10 weight ratio PCBM/BEH-PPV composite fibers: (a) digital image of as-spun BEH-PPV fibers with 1:10 weight ratio PCBM; (b–d) SEM micrographs of the BEH-PPV fibers doped with 1:10 weight ratio PCBM.

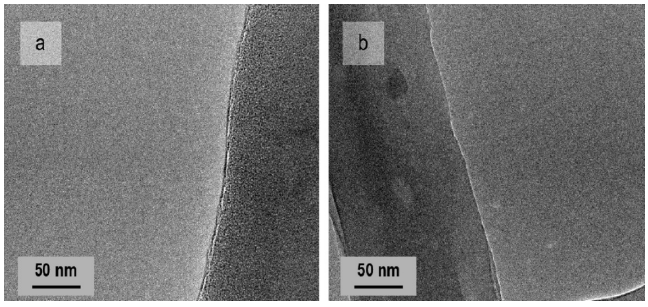

FIGURE 5. TEM of 1:10 weight ratio PCBM/BEH-PPV fibers.

15 cm at a flow rate of 2.0×10^{-2} mL/min. A digital image of the as-spun fibers with a 1:10 weight ratio loading of PCBM as a nonwoven mesh is shown in Figure 4a. In comparison to the pure BEH-PPV fibers, the 1:10 PCBM/BEH-PPV composite fibers exhibited a darker tint because of the presence of PCBM. The film properties were also similar to those of the pure BEH-PPV films and were easily handled and manipulated. Qualitative testing of the fibrous film with a black light also revealed evidence of quenching compared to the pure BEH-PPV fibers because of charge transfer from PPV to PCBM. SEM micrographs of these fibers are depicted in Figure 4b–d. The diameters of the electrospun fibers were uniform throughout and ranged from ~100 to 250 nm. There was little to no morphological difference between the fibers electrospun with and without PCBM. As with the neat BEH-PPV fibers, no beading was observed, although occasionally pores were seen upon the fiber surface, possibly from a phase separation that the polymer experienced during electrospinning. The ordered conformation of the polymer chains in the cosolvent system utilized may have led to a better distribution of PCBM within the polymer matrix and contributed to the lack of beading. Transmission electron microscopy (TEM) of these electrospun polymer fibers (Figure 5) did not reveal the typical signs of fullerene aggregations, which are commonly seen in composite films and are often represented by dark circular regions ranging from around 50 nm to several hundred nanometers (28). While further study is needed to ascertain the interactions in this composite, early indications reveal that the lack of

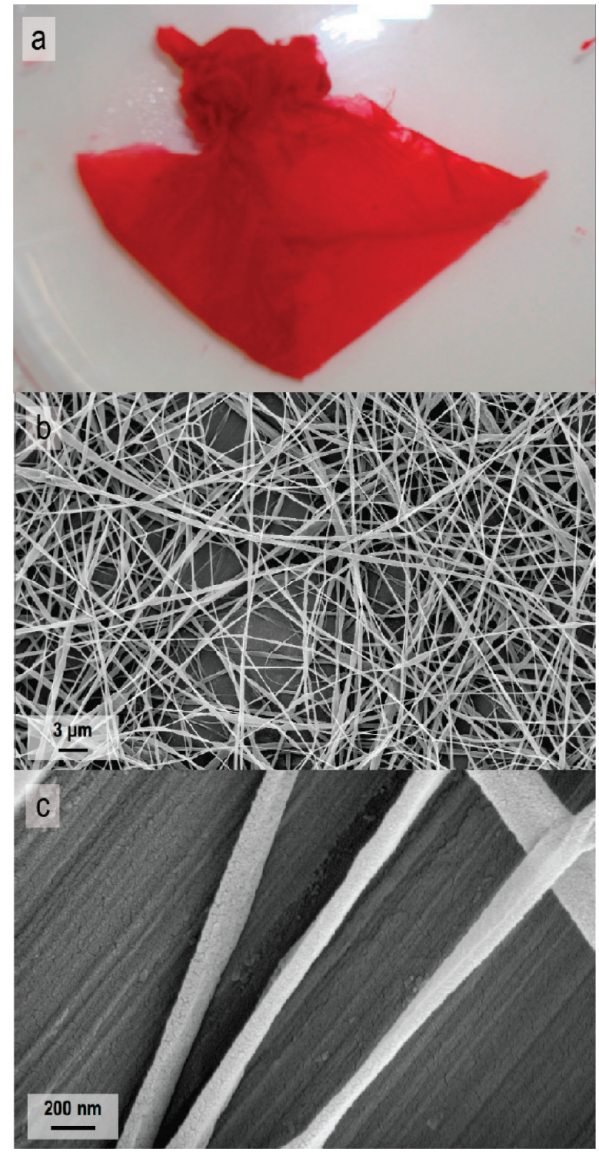

FIGURE 6. 1:3 PCBM/BEH-PPV composite fibers: (a) digital image of as-spun BEH-PPV fibers; (b and c) SEM micrographs of BEH-PPV fibers doped with PCBM.

these dark aggregates may be attributed to the process of electrospinning, which has been shown to align polymer chains, thus allowing for a more uniform dispersion of PCBM within the polymer matrix.

Composite polymer fibers containing a 1:3 weight ratio of PCBM/BEH-PPV were also fabricated through electrospinning with this solvent system. A digital image of the as-spun fibers is shown in Figure 6a. As seen with the 1:10 loading of PCBM, a darker tint was exhibited in the fibers because of the doping of BEH-PPV with PCBM. Even with the increased loading of fullerenes, the fibers were not brittle because of the crystalline nature of PCBM and were again easily handled and manipulated. The average diameter of the fibers was approximately 120 nm and was consistent throughout, with few or no signs of beading seen in all of the samples, although a more ribbonlike morphology was exhibited in some of the fibers. We again have attributed the spinability of this composite to the solvent system that was implemented, which allowed for a better alignment of

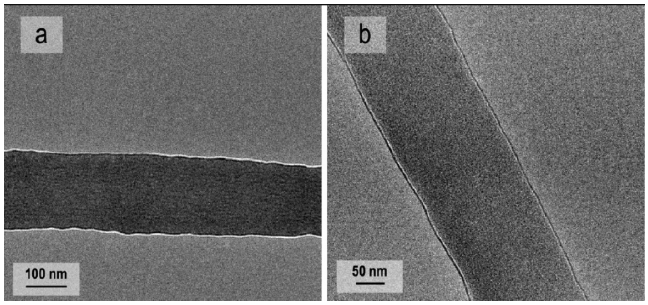

FIGURE 7. TEM of 1:3 PCBM/BEH-PPV fibers.

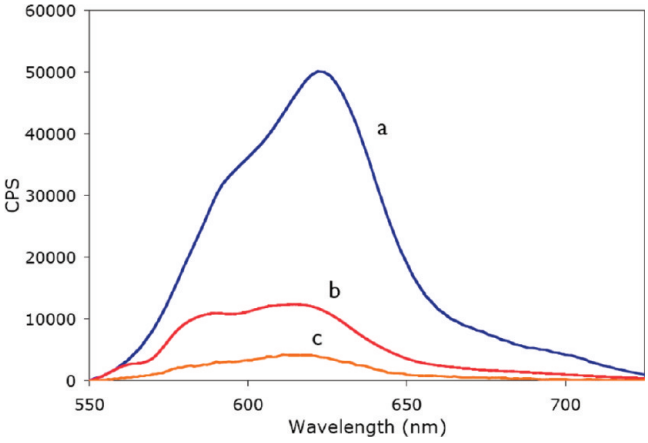

FIGURE 8. Fiber emission profiles of (a) BEH-PPV electrospun fibers, (b) PCBM/BEH-PPV (10:1, w/w) electrospun fibers, and (c) PCBM/BEH-PPV (1:3, w/w) electrospun fibers.

the polymer chains, as shown in the electrospinning of the pure polymer. The absence of the commonly seen dark spherical regions is again absent in the TEM images of the 1:3 weight ratio samples of PCBM/BEH-PPV electrospun fibers (Figure 7), which may indicate a lack of fullerene aggregation. The absence of any fullerene aggregation in the high loading of PCBM in the BEH-PPV fibers may lead to an increase of percolation pathways for the transport of holes and electrons, decreasing the occurrences of electron and hole recombination (39).

The emission profiles of the BEH-PPV composite fibers with 1:10 and 1:3 weight ratios of PCBM and BEH-PPV loading are depicted in Figure 8. The composite fibers with 1:10 loading show a profile with significantly lower emission even with a small loading, approximately 8.8% compared to that of the neat BEH-PPV fibers. This is due to the efficient photoinduced charge transfer from the polymer to the electron-accepting PCBM. The emission profile resembles the neat BEH-PPV fibers because of the low concentration of PCBM, although this trend is not seen when the loading is increased to a 1:3 weight ratio, where the emission is almost completely quenched, exhibiting an emission of approximately 1.1% that of the neat BEH PPV fibers. The process of electron transfer occurs in the subpicosecond range, faster than other competing processes (28, 50). This charge transfer consequently quenches the PL of the conjugated polymer, which is observed within our electrospun composite fibers.

To further test the efficacy of our solvent system, a 1:2 weight ratio of PCBM to BEH-PPV was studied and varying

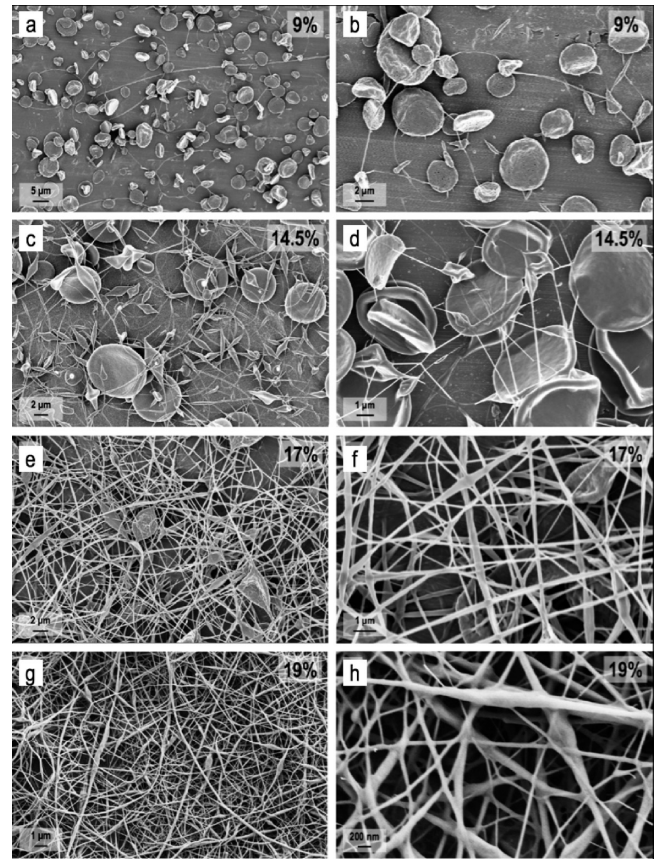

FIGURE 9. Effect of methanol on the spinability of the polymer melt: (a and b) 9% methanol; (c and d) 14% methanol; (e and f) 17% methanol; (g and h) 19% methanol.

solvent ratios were explored. To demonstrate the effect of methanol on the spinability of the polymer, the concentration of BEH-PPV in chloroform was kept constant while only methanol was varied. The amount of methanol used was varied from 0 to 19% of the total volume. The first signs of fiber formation were observed when the percent of methanol was raised to 9%, as can be seen from Figure 9a,b, although the majority of the sample exhibited signs of electrospraying. Previous attempts to electrospin the polymer solution at lower methanol concentrations showed few or no signs of elongation of the polymer solution and resulted in predominantly electrospraying. As the volume of methanol was increased in the solvent system, the frequency of electrospraying decreased dramatically and the initiation of fiber formation can be observed. At 14% of the total volume, the ratio of electrospraying to electrospinning is approximately equal (Figure 9c,d). The fibers formed at 14% methanol did, however, exhibit a leaflike, or a beaded morphology, likely because of the polymer chain conformation in solution and spinability of the polymer melt. As methanol was further increased to 17%, electrospraying was not observed and fibers were formed throughout the sample, although many of the fibers present large leaflike morphologies (Figure 9e,f). The optimal conditions for electrospinning of the sample of PCBM/BEH-PPV at a weight ratio of 1:2 were observed at 19%, where little to no beading occurred (Figure 9g,h). The majority of the fibers electrospun with this solvent ratio had a diameter of approximately 100

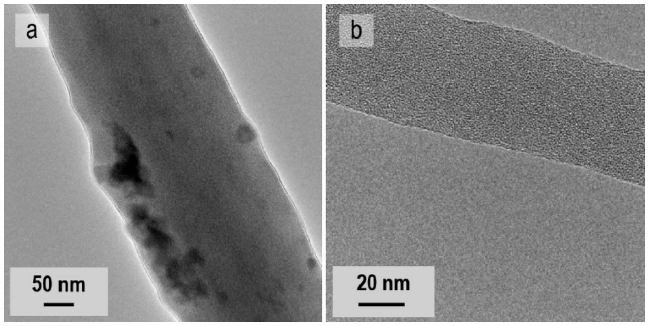

FIGURE 10. TEM of 1:2 PCBM/BEH-PPV fibers.

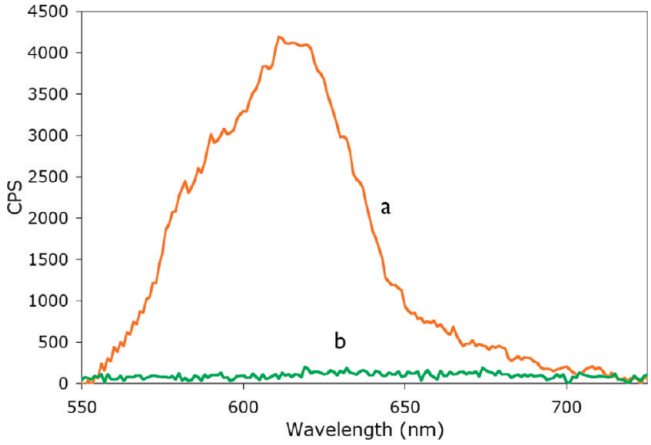

FIGURE 11. Fluorescence spectra of (a) 1:3 weight ratio PCBM-BEH PPV and (b) 1:2 weight ratio electrospun fibers.

nm, although many fibers exhibited much smaller diameters, some as small as 50 nm in diameter. In our study, a 1:2 weight ratio was the highest loading of PCBM that was achieved and further attempts to increase the amount of fullerenes in the polymer did not result in fiber formation.

Further analysis of the fibers through TEM revealed the first indications of possible fullerene aggregation within the polymer matrix similar to those seen in previous studies (Figure 10a) (51). Aggregations of the fullerenes typically appeared as either large, dark clusters of approximately 50 nm in length or small circular collections of approximately 20 nm in diameter, which were occasionally observed. While some aggregation was expected at such a high loading, the majority of the fibers did not display these dark clusters within the polymer fibers (Figure 10b), alluding to a homogeneous blend between PCBM and BEH PPV. PL spectra of the PCBM/BEH-PPV electrospun fibers in a 1:2 weight ratio are shown in comparison to the 1:3 weight ratio emission profiles in Figure 11. The emission of the fibers with the high loading of PCBM displayed complete quenching of the PL resulting from the charge transfer between the conjugated polymer and the fullerene derivative.

CONCLUSION

In conclusion, we have electrospun neat uniform BEH-PPV fibers with diameters ranging from ~100 to 300 nm without the need for copolymer or surfactant. We have also demonstrated that electrospinning with the proposed solvent system leads to the alignment of the polymer chains and an increase in the interchain interaction within the pure polymer fibers through PL data. Composite fibers of BEH-PPV and PCBM have also been electrospun and exhibit a good dispersion with few signs of PCBM aggregation.

While the quenching of PL gives evidence of electron transfer, this may also indicate the fullerene action as a carrier trap, which may prove to be detrimental in the long-range transport of charge. Thus, future studies will include conductivity measurements to test the charge mobility of the fibers to determine if this method of fabrication improves charge percolation pathways. Additionally, blends of BEH-PPV with other electron acceptors are also being explored in order to tune the electronic and optoelectronic properties for PLEDs.

EXPERIMENTAL SECTION

Materials. All chemicals and solvents were obtained from Aldrich Chemical Co. and were used as received unless otherwise noted. Potassium *tert*-butoxide was sublimed at 160 °C and 0.05 mmHg and was stored in a nitrogen-filled glovebox. Tetrahydrofuran (THF) was dried using an MBraun SP Series solvent purification system. The water content (<20 ppm) was determined with a Karl-Fisher titrator (Denver Instruments, model 270). All reagents were used as received unless otherwise stated. [6,6]-Phenyl-C_{61}-butyric acid methyl ester (PCBM) was purchased from American Dye Source, Inc.

Characterization Methods. The morphology of the fibers was evaluated by scanning electron microscopy (SEM) using a LEO 1530 VP field-emission electron microscope from gold/palladium-coated samples. TEM of the electrospun BEH-PPV/PCBM composite fibers was performed with an FEI CM200 FEG transmission electron microscope operating at 200 kV. TEM sample preparation was done by placing the TEM grid on the grounded collecting plate and electrospinning for approximately 30 s. ^{1}H and ^{13}C NMR spectra were obtained using a JEOL FX-270 MHz spectrometer using deuterated chloroform with tetramethylsilane as an internal standard. Molecular weights were obtained via gel permeation chromatography (GPC) using THF as the eluent. Experiments were done on two ViscoGel I-Series (I-MBHMW-3078) columns with a Viscotek 302 triple array detector (TDA 302: refractometer, light scattering, and viscometer). Narrow polystyrene standards were used for calibration. Data were analyzed using Viscotek OmniSEC software, version 3.0. UV−visible absorption spectra were collected using a Shimadzu UV-1601PC UV−visible spectrophotometer controlled by UV-1601PC software. Emission spectra were collected using a Jobin−Yvon fluorimeter controlled by Datamax software, version 1.03.

BEH-PPV. The BEH-PPV monomer and its polymer were synthesized following reported procedures (35) with the following modifications.

Synthesis of 1,4-Bis(2′-ethylhexyloxy)benzene. Potassium hydroxide (509 mmol) was dissolved in dimethyl sulfoxide (DMSO; 150 mL) in a 250 mL, three-neck, round-bottomed flask under a blanket of nitrogen. Hydroquinone (182 mmol) was then added, and the mixture was stirred for 0.5 h at room temperature, followed by the addition of 2-ethylhexyl bromide (478 mmol). The reaction was stirred under nitrogen at room temperature overnight. The organic layer was separated and washed three times with 100 mL of deionized water. The organic layers were combined and dried over magnesium sulfate. The solvent was removed under reduced pressure, and the residue was purified by column chromatography (basic alumina, hexanes) to afford 47 g (78% yield) of yellow oil. ^{1}H NMR ($CDCl_3$, 270 MHz): δ 6.86 (s, 4H, $C^{ar}H$), 3.84−3.81 (d, 4H, OCH_2), 1.8−1.65 (m, 2H, OCH_2CH), 1.6−1.2 (m, 18H, other

CH_2), 0.97−0.95 (t, 12H, CH_3). ^{13}C NMR ($CDCl_3$, 270 MHz): δ 153.5 (s, $C^{ar}O$), 115.4 (s, $C^{ar}H$), 71.2 (s, OCH_2), 39.6 (s, OCH_2CH), 30.6 (s, CH_2), 28.9, 23.9, 23.2 (s, CH_2), 14.2 (s, CH_3), 11.2 (s, other CH_3).

Synthesis of 1,4-Bis(bromomethyl)-2,5-bis(2′-ethylhexyloxy)-benzene. 1,4-Bis(2-ethylhexyloxy)benzene (135 mmol) was added to a suspension of paraformaldehyde (19.4 g, 647 mmol) and glacial acetic acid (25 mL) in a 250 mL, round-bottomed flask. The suspension was stirred for 15 min at room temperature, and then 117 mL of 33% HBr in acetic acid (646 mmol) was added at once. The reaction was then heated to reflux at 80 °C for 5 h. The reaction mixture was cooled to room temperature, and a crude product was partitioned between water and chloroform. The aqueous layer was back-extracted with chloroform and the organic phase washed with 7% sodium carbonate (3×). The organic phase was dried over magnesium sulfate, followed by removal of the solvent under reduced pressure. Crystallization from isopropyl alcohol afforded 23 g (42% yield). Mp: 63.5−65 °C. ^1H NMR ($CDCl_3$, 270 MHz): δ 6.84 (s, 2H, $C^{ar}H$), 4.51 (s, 4H, CH_2Br), 3.91−3.82 (d, 4H, OCH_2), 1.8−1.65 (m, 2H, OCH_2CH), 1.6−1.20 (m, 18H, CH_2), 0.97−0.94 (t, 12H, CH_3). ^{13}C NMR ($CDCl_3$, 270 MHz): δ 138.3 (s, $C^{ar}C$), 150.7 (s, $C^{ar}O$), 127.4 (s, $C^{ar}H$), 115 (s, $C^{ar}C$), 71.2 (s, OCH_2), 39.6 (s, OCH_2CH), 30.7 (s, CH_2), 29.2, 24.1, 23.1 (s, CH_2), 14.2 (s, CH_3), 11.1 (s, other CH_3).

Poly[2,5-(2′-ethylhexyloxy)]-1,4-phenylenevinylene (BEH-PPV). Weighing and transfer of the reagents were performed inside a nitrogen-filled glovebox. Potassium *tert*-butoxide (1.0 g, 9.2 mmol) and *p*-methoxyphenol (6.7 mg, 2.5 mol %) were added to a 250 mL flask, and these were dissolved in anhydrous THF (120 mL). The flask was removed from the glovebox, and an IKA Eurostar mechanical stirrer was attached, keeping the flask flushed with nitrogen. The mixture was stirred at 300 rpm while cooling the flask in an isopropyl alcohol/liquid-nitrogen bath (−35 °C). BEH-PPV monomer (1.0 g, 1.9 mmol) was dissolved in anhydrous THF (20 mL) and was injected at a rate of 20 mL/h using a KDS (series 200) syringe pump. Stirring and cooling was continued for 1 h after the monomer addition was complete. The red polymer was precipitated in methanol, collected on a Millipore Durapore 0.45 μm membrane filter, and dried under vacuum overnight at 50 °C. The polymer was then dissolved in THF and precipitated in methanol three times. The red polymer strands were collected and dried under vacuum to give 0.61 g (88% yield) of BEH-PPV. ^1H NMR (270 MHz, $CDCl_3$): δ 7.75−7.41 (d, 1.2H), 4.27−3.75 (t, 4H), 1.93−1.73 (t, 2H), 1.70−0.45 (m, 28H). UV−visible absorption ($CHCl_3$): λ_{max} 505 nm. Emission ($CHCl_3$): λ_{max} 557 nm. GPC (THF): M_w = 217 kDa; PDI = 1.7. FT-IR (polymer film) (cm^{-1}): 472, 723, 772, 1586, 1692, 1804, 1830, 2031, 2221, 2316, 2601, 2668, 2731, 2974.

Preparation of Polymer Solutions. Solutions of BEH-PPV at a concentration of 3% (w/v) were first prepared in chloroform under vigorous stirring until a uniform polymer solution was attained. Then methanol was added with vigorous stirring, resulting in a chloroform to methanol ratio of 5:1 (v/v). For samples doped with PCBM, PCBM was first dispersed in chloroform and sonicated for 30 min, resulting in a dark-purple solution. BEH-PPV in chloroform was then added to this solution in the appropriate ratio and further stirred vigorously until homogeneous. To this solution, methanol was added in varying ratios ranging from 1:5 to 1:6.

Electrospinning of BEH-PPV and Composite Materials. In a typical electrospinning procedure, the as-prepared solution was loaded in a 10 mL plastic syringe equipped with a 22 gauge flat-tipped stainless steel needle. The electrospinning was initiated when a voltage of 10−15 kV was applied to the needle tip using a variable high-voltage power supply (ES50P-5W, Gamma High Voltage Research). The fibers were collected on a grounded rotating drum covered with aluminum foil positioned a distance of 20 cm from the needle. The flow rate varied depending on the polymer solution and ranged from 0.05 to 0.01 mL/min.

Acknowledgment. We acknowledge Chalita Ratanatawanate for help with the gathering of TEM images. This material is based upon work funded by the Robert A. Welch Foundation and by CONTACT.

REFERENCES AND NOTES

(1) Reneker, D. H.; Chun, I. *Nanotechnology* **1996**, *7* (3), 216–223.
(2) Reneker, D. H.; Yarin, A. L. *Polymer* **2008**, *49*, 2387–2425.
(3) Li, D.; Wang, Y.; Xia, Y. *Nano Lett.* **2003**, *3*, 1167–1171.
(4) Macias, M.; Chacko, A.; Ferraris, J. P.; Balkus, K. J., Jr. *Microporous Mesoporous Mater.* **2005**, *86*, 1–13.
(5) Madhugiri, S.; Sun, B.; Smirniotis, P. G.; Ferraris, J. P.; Balkus, K. J., Jr. *Microporous Mesoporous Mater.* **2004**, *69*, 77–83.
(6) Li, D.; Xia, Y. *Nano Lett.* **2003**, *3*, 555–560.
(7) Viswanathamurthi, P.; Bhattarai, N.; Kim, H. Y.; Lee, D. R.; Kim, S. R.; Morris, M. A. *Chem. Phys. Lett.* **2003**, *374*, 79–84.
(8) Sigmund, W.; Yuh, J.; Park, H.; Maneeratana, V.; Pyrgiotakis, G.; Daga, A.; Taylor, J.; Nino, J. C. *J. Am. Ceram. Soc.* **2006**, *89*, 395–407.
(9) Yuh, J.; Nino, J. C.; Sigmund, W. M. *Mater. Lett.* **2005**, *59*, 3645–3647.
(10) Balkus, K. J.; Ferraris, J. P.; Madhugiri, S. U.S. Patent 7,390,452, 2008.
(11) Balkus, K. J.; Ferraris, J. P.; Madhugiri, S.; Scott, A. S. U.S. Patent Appl. 2004 0137225.
(12) Kang, T. S.; Lee, S. W.; Joo, J.; Lee, J. Y. *Synth. Met.* **2005**, *153*, 61–64.
(13) Norris, I. D.; Shaker, M. M.; Ko, F. K.; MacDiarmid, A. G. *Synth. Met.* **2000**, *114*, 109–114.
(14) Zhou, Y.; Freitag, M.; Hone, J.; Staii, C.; Johnson, A. T., Jr.; Pinto, N. J.; MacDiarmid, A. G. *Appl. Phys. Lett.* **2003**, *83*, 3800–3802.
(15) Huang, Z. M.; Zhang, Y. Z.; Kotaki, M.; Ramakrishna, S. *Compos. Sci. Technol.* **2003**, *63*, 2223–2253.
(16) Khanam, N.; Mikoryak, C.; Draper, R. K.; Balkus, K. J., Jr. *Acta Biomater.* **2007**, *3*, 1050–1059.
(17) Yoshimoto, H.; Shin, Y. M.; Terai, H.; Vacanti, J. P. *Biomaterials* **2003**, *24*, 2077–2082.
(18) Jia, H.; Zhu, G.; Vugrinovich, B.; Kataphinan, W.; Reneker, D. H.; Wang, P. *Biotechnol. Prog.* **2002**, *18*, 1027–1032.
(19) Kim, C.; Ngoc, B. T. N.; Yang, K. S.; Kojima, M.; Kim, Y. A.; Kim, Y. J.; Endo, M.; Yang, S. C. *Adv. Mater.* **2007**, *19*, 2341–2346.
(20) Kim, C.; Yang, K. S.; Lee, W. J.*Electrochem. Solid-State Lett.* **2004**, 7.
(21) Kenawy, E. R.; Bowlin, G. L.; Mansfield, K.; Layman, J.; Simpson, D. G.; Sanders, E. H. *J. Controlled Release* **2002**, *81*, 57–64.
(22) Liu, H. A.; Gnade, B. E.; Balkus, K. J., Jr. *Adv. Funct. Mater.* **2008**, *18*, 3620–3629.
(23) Anton, F. Method and apparatus for spinning. U.S. Patent 2,349,950, 1944.
(24) Reneker, D. H.; Yarin, A. L.; Fong, H.; Koombhongse, S. *J. Appl. Phys.* **2000**, *87*, 4531–4547.
(25) Jaeger, R.; Schonherr, H.; Vancso, G. J. *Macromolecules* **1996**, *29*, 7634–7636.
(26) Li, D.; Babel, A.; Jenekhe, S. A.; Xia, Y. *Adv. Mater.* **2004**, *16*, 2062–2066.
(27) Pedicini, A.; Farris, R. J. *Polymer* **2003**, *44*, 6857–6862.
(28) Hoppe, H.; Sariciftci, N. S. *J. Mater. Chem.* **2006**, *16*, 45–61.
(29) Schwartz, B. J. *Annu. Rev. Phys. Chem.* **2003**, *54*, 141–172.
(30) Hoofman, R. J. O. M.; de Haas, M. P.; Siebbeles, L. D. A.; Warman, J. M. *Nature* **1998**, *392*, 54.
(31) Nguyen, T.-Q.; Wu, J.; Doan, V.; Schwartz, B. J.; Tolbert, S. H. *Science* **2000**, *288*, 652–656.
(32) Colvin, V. L.; Schlamp, M. C.; Alivisatos, A. P. *Nature* **1994**, *370*, 354–357.
(33) Greenham, N. C.; Moratti, S. C.; Bradley, D. D. C.; Friend, R. H.; Holmes, A. B. *Nature* **1993**, *365*, 628–630.
(34) Chasteen, S. V.; Sholin, V.; Carter, S. A.; Rumbles, G. *Sol. Energy Mater. Sol. Cells* **2008**, *92*, 651–659.
(35) Neef, C. J.; Ferraris, J. P. *Macromolecules* **2000**, *33*, 2311–2314.
(36) Kraft, A.; Grimsdale, A. C.; Holmes, A. B. *Angew. Chem., Int. Ed.* **1998**, *37*, 402–428.
(37) Hoppe, H.; Sariciftci, N. S. *J. Mater. Res.* **2004**, *19*, 1924–1945.

(38) Mozer, A. J.; Denk, P.; Scharber, M. C.; Neugebauer, H.; Sariciftci, N. S.; Wagner, P.; Lutsen, L.; Vanderzande, D. *J. Phys. Chem. B* **2004**, *108*, 5235–5242.
(39) Hoppe, H.; Glatzel, T.; Niggemann, M.; Schwinger, W.; Schaeffler, F.; Hinsch, A.; Lux-Steiner, M. C.; Sariciftci, N. S. *Thin Solid Films* **2006**, *511–512*, 587–592.
(40) Madhugiri, S.; Dalton, A.; Gutierrez, J.; Ferraris, J. P.; Balkus, K. J., Jr. *J. Am. Chem. Soc.* **2003**, *125*, 14531–14538.
(41) Washington, A. L., Jr. Ph.D. Dissertation. The University of Texas at Dallas, Richardson, TX, 2007.
(42) Zhang, W.; Yan, E.; Huang, Z.; Wang, C.; Xin, Y.; Zhao, Q.; Tong, Y. *Eur. Polym. J.* **2007**, *43*, 802–807.
(43) Zhao, Q.; Xin, Y.; Huang, Z.; Liu, S.; Yang, C.; Li, Y. *Polymer* **2007**, *48*, 4311–4315.
(44) Kraabel, B.; Hummelen, J. C.; Vacar, D.; Moses, D.; Sariciftci, N. S.; Heeger, A. J.; Wudl, F. *J. Chem. Phys.* **1996**, *104*, 4267–4273.
(45) Collison, C. J.; Rothberg, L. J.; Treemaneekarn, V.; Li, Y. *Macromolecules* **2001**, *34*, 2346–2352.
(46) Hu, D.; Yu, J.; Wong, K.; Bagchi, B.; Rossky, P. J.; Barbara, P. F. *Nature* **2000**, *405*, 1030–1033.
(47) Zheng, M.; Bai, F.; Zhu, D. *Polym. Adv. Technol.* **1999**, *10*, 476–480.
(48) Nguyen, T.-Q.; Martini, I. B.; Liu, J.; Schwartz, B. J. *J. Phys. Chem. B* **2000**, *104*, 237–255.
(49) Traiphol, R.; Sanguansat, P.; Srikhirin, T.; Kerdcharoen, T.; Osotchan, T. *Macromolecules* **2006**, *39*, 1165–1172.
(50) Hoppe, H.; Niggemann, M.; Winder, C.; Kraut, J.; Hiesgen, R.; Hinsch, A.; Meissner, D.; Sariciftci, N. S. *Adv. Funct. Mater.* **2004**, *14*, 1005–1011.
(51) Martens, T.; D'Haen, J.; Munters, T.; Beelen, Z.; Goris, L.; Manca, J.; D'Olieslaeger, M.; Vanderzande, D.; De Schepper, L.; Andriessen, R. *Synth. Met.* **2003**, *138*, 243–247.

AM900338W